Inorganic Chemistry

ARTICLE

pubs.acs.org/IC

New Cyclopentenyl-Linked [NPN] Ligands and Their Coordination Chemistry with Zirconium: Synthesis of a Dinuclear Side-On-Bound Dinitrogen Complex

Ting Zhu, Truman C. Wambach, and Michael D. Fryzuk*

Department of Chemistry, The University of British Columbia, 2036 Main Mall, Vancouver, British Columbia, Canada V6T 1Z1

Supporting Information

ABSTRACT: The synthesis and characterization of two 1,2-cyclopentyl-bridged diiminophosphine proligands, $^{CY5}[NPN]^{DMP}H_2$ (CY5 = cyclopentylidene; DMP = 2,6-$Me_2C_6H_3$) and $^{CY5}[NPN]^{DIPP}H_2$ (DIPP = 2,6-$^{i}Pr_2C_6H_3$), are presented, and tautomerization to the corresponding 1,2-cyclopentenyl-bridged enamineimine phosphine precursors is reported. These two new proligands are obtained by deprotonation of *N*-DMP- or *N*-DIPP-cyclopentylideneimine (*N*-DMP, 2,6-dimethylphenyl; *N*-DIPP, 2,6-diisopropylphenyl) and the subsequent addition of 0.5 equiv of dichlorophenylphosphine. Each ligand precursor exists as a mixture of isomers that consist of the diimine, enamineimine, and dienamine tautomers and corresponding stereoisomers, each of which could be identified. The bis(dimethylamido)zirconium complexes $^{CY5}[NPN]^{DMP}Zr(NMe_2)_2$ and $^{CY5}[NPN]^{DIPP}Zr(NMe_2)_2$ were prepared directly from the neutral proligands and $Zr(NMe_2)_4$ via protonolysis. Exchange of the dimethylamido ligands in the latter complexes for chlorides and iodides takes place upon reaction with excess Me_3SiCl and Me_3SiI, respectively. A dinuclear zirconium−dinitrogen complex, $\{^{CY5}[NPN]^{DMP}Zr(THF)\}_2(\mu-\eta^2:\eta^2\text{-}N_2)$, was obtained via KC_8 reduction of $^{CY5}[NPN]^{DMP}ZrCl_2$ under 4 atm of N_2. On the basis of single-crystal X-ray analysis, N_2 has been reduced to a side-on-bound hydrazido ($\mu\text{-}\eta^2:\eta^2\text{-}N_2^{4-}$) unit. This dinitrogen complex is thermally unstable and decomposes in solution.

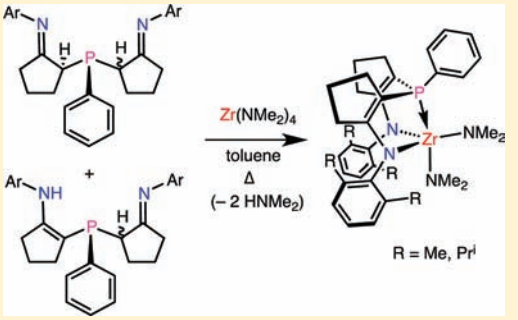

INTRODUCTION

Amidophosphine hybrid ligands are multidentate ligand scaffolds that incorporate hard amido and soft phosphine donors in various permutations.[1−9] We have already reported[10−19] a number of combinations with $-CH_2SiMe_2-$ linking units, as shown generically coordinated to metals in Chart 1.

Depending on the charge of the ligand donor set, a variety of oxidation states and coordination geometries can be accessed. Of recent interest in our group have been the diamidophosphine arrays (NPN), which have shown a rich chemistry in small-molecule activation.[6,18,20−29] We have explored NPN derivatives with different linker units ranging from the original $-CH_2SiMe_2-$ (**A**) to *o*-phenylene (**B**) and 2,3-thiophene (**C**), as shown in Chart 2.

In an effort to simplify the synthesis of these kinds of systems, we designed a new 1,2-alkenyl-linked NPN ligand framework. In Scheme 1, the rationale is given graphically. To avoid the kinetically labile Si−N bond found in **A**, we have explored robust C−N and C−P bonds, especially those involving sp^2 hybridization, as is evident from our studies on the already mentioned *o*-phenylene-linked NPN system (**B**)[4,26] and the analogous 2,3-thiophene-linked system (**C**),[6] both of which use Hartwig−Buchwald arylamination procedures to generate the C−N bond. Common to both **B** and **C** is the dienamidophosphine linker shown as **D**, but rather than examine this unsubstituted system, a more convenient precursor to use was the cyclopentylidene−ketoimine precursor (**E**), which ensures that the imine and phosphine donors have a syn orientation; the use of condensation chemistry to generate the imine unit also simplifies the formation of the C−N bond. The imine unit has figured prominently

Chart 1

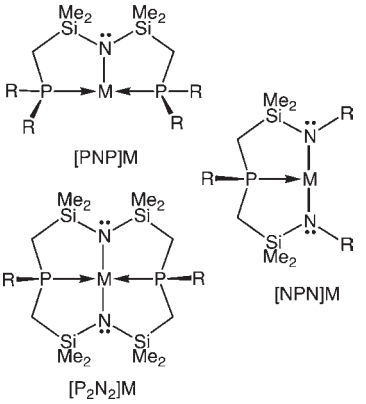

Received: August 13, 2011
Published: October 07, 2011

dx.doi.org/10.1021/ic201762r | *Inorg. Chem.* 2011, 50, 11212–11221

Chart 2

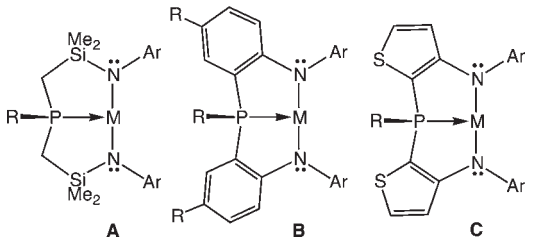

Scheme 1

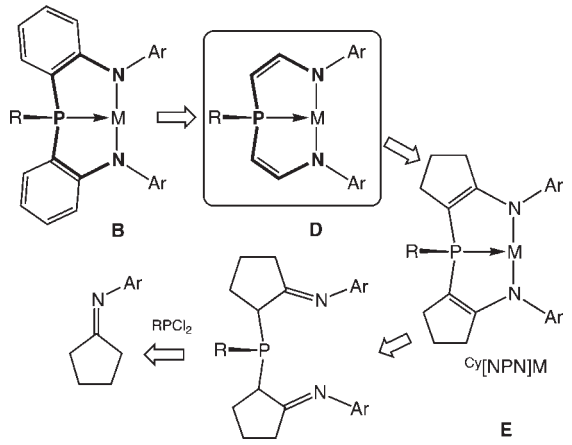

recently with a number of studies on diiminopyridine-type ligands and their coordination chemistry with a variety of metals;[30−39] there have also been reports of chelating iminophosphine ligands and their coordination chemistry with iron.[40−43] This paper documents the synthesis of a diiminephosphine precursor framework starting from arylimine derivatives of cyclopentanone and its coordination chemistry with zirconium. We also report the formation of a thermally labile dinuclear dinitrogen complex of zirconium formed via reduction using KC_8.

RESULT AND DISCUSSION

Synthesis of ^{CY5}[NPN]^{DMP}H$_2$ (1a) and ^{CY5}[NPN]^{DIPP}H$_2$ (1b). Our short-form descriptors for these ligand precursors use the linker ring CY5 for the cyclopentylidene unit and either DMP or DIPP to indicate the substitution pattern of the *N*-arylimine moiety, with DMP being 2,6-dimethylphenyl and DIPP short for 2,6-diisopropylphenyl. These ligands can be easily assembled using a modification of a literature preparation.[44] The reaction of either cyclopentylidene−2,6-dimethylaniline or cyclopentylidene−2,6-diisopropylaniline with lithium diisopropylamide (LDA) at low temperature followed by quenching with 0.5 equiv of dichlorophenylphosphine results in the formation of the diiminephosphine derivatives **1a** and **1b**, as shown in eq 1. The original literature preparation[44] describes the synthesis of bidentate P,N ligands and reports the use of BuLi as the preferred method of generating the enamide via deprotonation of an α-methylene proton of the cyclopentylidene ketoimine. However,

Scheme 2

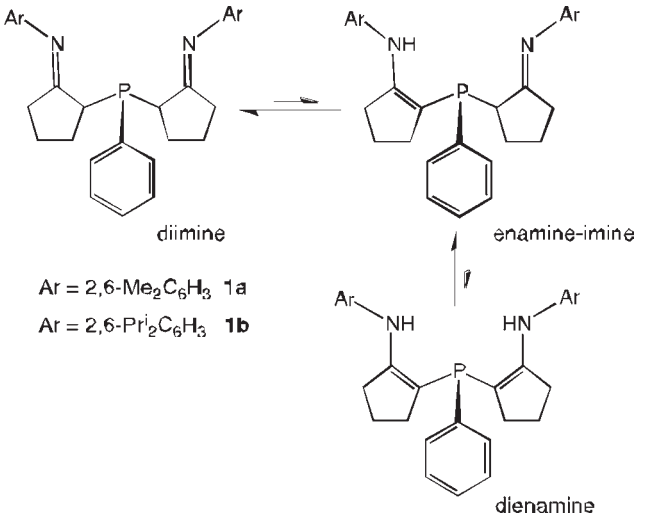

we found that this method was not reliable, and so we opted for the LDA deprotonation protocol instead.

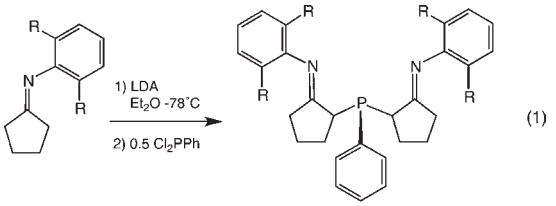

From these reactions, one could isolate oily, yellow materials that were mixtures of products; for both **1a** and **1b**, five singlets were initially observed in the ^{31}P NMR spectrum, corresponding to five different species, in variable amounts (see the Experimental Section). We could purify the oily mixtures to generate solids by rapid precipitation from a pentane solution; in the case of **1a**, depending on the workup, the solid could be either a mixture of five species in similar amounts to the crude oily mixture or just one pure compound. For **1b**, a single compound with $\delta(^{31}P\{^1H\})$ −8.8 was isolated as a powder in moderate yield and identified as the diiminophosphine proligand by ^{1}H NMR spectroscopy ($^1H\{^{31}P\}$ NMR), mass spectrometry (EI-MS), and elemental analysis (EA); that the diimine tautomer of **1b** was isolated was ascertained by HSQC spectroscopy because each proton resonance correlates to a ^{13}C signal and therefore indicates the absence of NH protons. On the basis of NMR spectroscopy, we were able to definitively assign this material as a *meso*-diimine stereoisomer of **1b**, which was confirmed via X-ray analysis (vide infra).

As was observed for the related bidentate systems, the existence of isomers is likely due, in part, to a tautomeric equilibrium between the imine and enamine forms; however, in our case, because we have two imines linked by a tertiary phosphine, there exist stereoisomers as well as structural isomers, the latter being due to the aforementioned equilibrium. This is shown generically in Scheme 2 and could potentially involve the diimine, enamineimine, and dienamine tautomers. As will be discussed below,

dx.doi.org/10.1021/ic201762r |*Inorg. Chem.* 2011, 50, 11212–11221

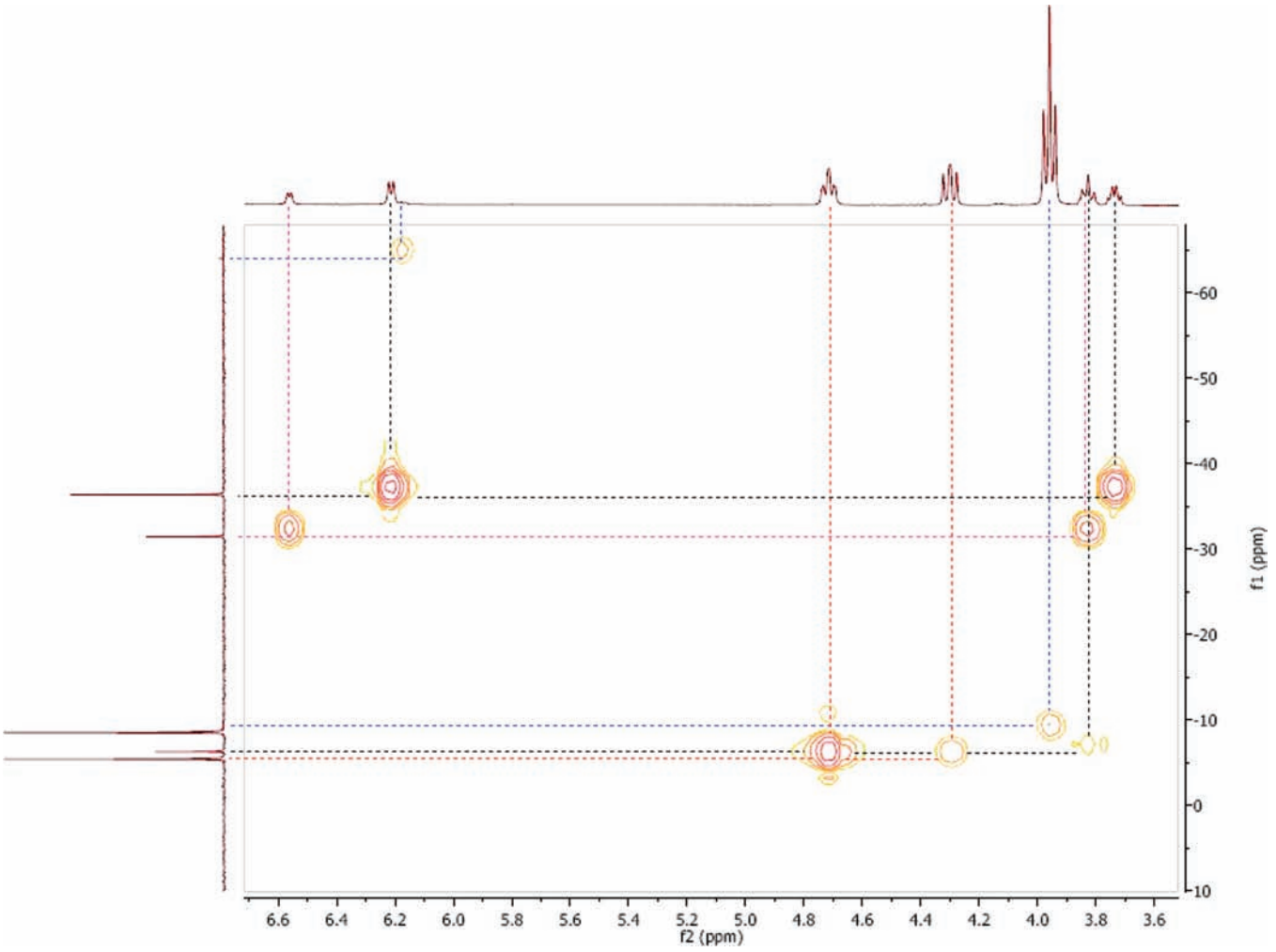

Figure 1. ^{31}P HMBC NMR at 400 MHz taken in C_6D_6.

there could potentially be six isomeric species formed: three diastereomeric forms of the diimine (two *meso* and one *rac*), two diastereomeric enamineimines, and the dienamine. Given that we could see five species initially, one of the challenges was to determine if indeed a sixth species was formed and, if so, to locate its resonance in the ^{31}P NMR spectrum.

For the DMP ligand precursor **1a**, dissolution of the solid material obtained from pentane in C_6D_6 showed five peaks in the ^{31}P NMR spectrum at δ −5.6 (28%), −6.0 (6%), −8.5 (47%), −32.1 (6%), and −36.7 (13%); the actual amounts of each material vary by a few percent, but the major product is always the peak at δ −8.5. By use of a series of 2D NMR experiments, these resonances could be assigned. In Figure 1, the ^{31}P HMBC NMR spectrum of the mixture shows that the major peak at δ −8.5 only correlates with the triplet at δ 3.9 in the ^{1}H NMR spectrum; the other two peaks in this part of the ^{31}P NMR spectrum (i.e., at δ −5.6 and −6.0) also correlate to peaks between δ 5.0 and 3.6 in the ^{1}H NMR spectrum; as will be shown below, these ^{1}H NMR peaks are due to the α protons next to the phosphine in the cyclopentyl substituent and are assigned to the *rac* and two *meso* forms of the dimine tautomer. Another set of resonances in the ^{31}P NMR spectrum are the upfield peaks at δ −32.1 and −36.7; using ^{31}P HMBC NMR, these two resonances correlate with two small doublets between δ 6.6 and 6.2, as well as the α protons of the cyclopentyl unit in the ^{1}H NMR spectrum. The two small doublets arise from N−H protons of the enamineimine tautomers, which was determined from the ^{13}C HSQC NMR experiment that showed no correlation of these two doublets with any carbon atoms in the ^{13}C NMR spectrum. Thus, the two upfield singlets in the ^{31}P NMR spectrum (δ −32.1 and −36.7) are due to enamineimine tautomers, and there are two diastereomers that result from the stereogenic phosphorus and carbon centers in this tautomeric form (Chart 3). The doublets arise from long-range coupling to the phosphine ($^{4}J_{NP} \sim 4-6$ Hz).

At this point, the five species identified consist only of diimine and enamineimine forms of **1a**, with no peaks attributable to the dienamine tautomer. On the basis of the upfield shift of the enamineimine form compared to the diimine, we reasoned that the ^{31}P NMR resonance for the putative dienamine species would likely be located upfield of the enamineimine form, likely in the range of δ −60 to −70. Upon close examination of this region, we did find a very small resonance at δ −63, which correlated in the ^{31}P HMBC NMR experiment to a shoulder in the N−H region of the ^{1}H NMR spectrum at δ 6.2. This is shown in Figure 1.

As was already mentioned, the major peak in the ^{31}P NMR spectrum of **1a** occurs at δ −8.5 and correlates to a single CH

dx.doi.org/10.1021/ic201762r |*Inorg. Chem.* 2011, 50, 11212–11221

Chart 3

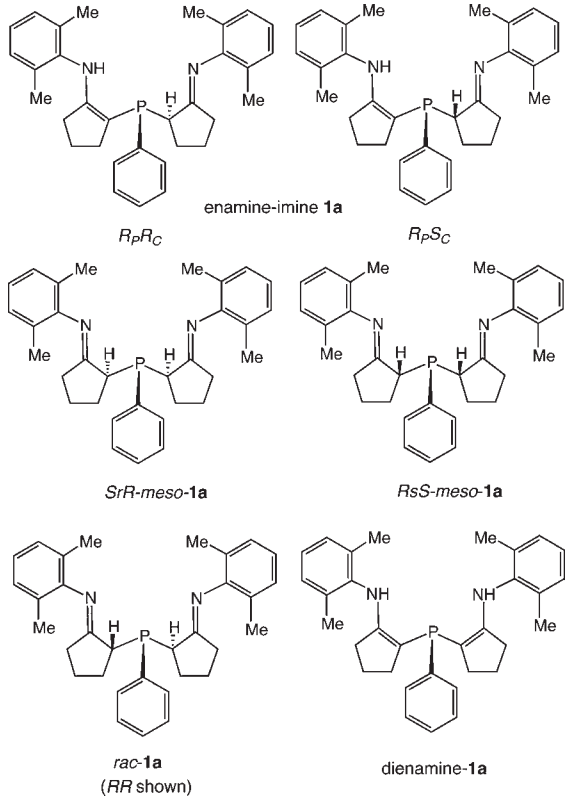

resonance at δ 3.9; this identifies it as a *meso* diastereomer of the diimine tautomer of the ligand, which has been confirmed by X-ray crystallography (vide infra). A second diastereomer of the diimine tautomer of the ligand is assigned to a ^{31}P resonance at δ −5.4. This signal correlates with two CH protons, supporting the assignment of this resonance as the *rac* stereoisomer of the diimine tautomer of the ligand. As illustrated in Chart 3, the two α protons of the *rac* enantiomers (*RR* and *SS*) are not related by symmetry; therefore, two unique resonances would be expected in the ^{1}H NMR spectrum. The α protons of both *meso* diastereomers are related by a mirror plane and thus appear as a single resonance.

In the mixture of isomers of **1a**, the ^{31}P resonance at δ −6.0 (∼6−7% of the mixture) is a second *meso* diastereomer, which is predicted to be present due to the pseudochiral phosphorus center; this signal is very close to the resonances of the *rac*- and *meso*-dimine diastereomers, which is consistent with a diimine framework because the chemical shift is consistent with sp^3 hybridization of both α-carbons of the cyclopentyl linker that flank the ^{31}P nucleus. A single cross peak is observed by ^{31}P HMBC NMR in the region of interest; this ^{31}P resonance correlates with a ^{1}H signal at δ 3.8, which overlaps with the previously discussed resonances assigned as α-CH protons.

The single-crystal X-ray structures of the major isomers of both ligand precursors have been determined. X-ray-quality crystals of **1a** were obtained by dissolving the crude mixture in boiling methanol followed by slow cooling of the solution. The crystal selected was partially oxidized at the phosphorus center; this partial oxidation was modeled as a disordered oxygen atom with 12.8% occupancy. The solid-state molecular structure is shown in Figure 2, along with selected bond lengths and angles. What is clearly evident is that the crystal is the dimine tautomer and that it is the *meso* diastereomer, with the *SrR* absolute configuration. All of the distances and angles are that expected for this dimine form with two C=N double bonds and sp^3-hybridized α-carbon centers. One notable feature of the structure is a short contact, perhaps due to hydrogen bonding, between the α-CH bond and the distal imine nitrogen, H7 and N1 [H7···N1, 2.55(3) Å].

X-ray-quality crystals of **1b** were obtained by recrystallization of the crude powder from hexanes; the solid-state structure is given in the Supporting Information (Figure S3). There were no indicators of partial oxidation in the solid-state molecular structure obtained for **1b**. It is also the diimine form and is the (*SrR*)-*meso* diastereoisomer. The bond lengths and angles of **1b** are very similar to those of **1a**, as expected. No short contacts are observed between N1 and H7 in this iteration of the ligand, likely because of the presence of the increased steric bulk of the 2,6-diisopropyl substituents on the arylimines, which prevents a conformation that orients the imine nitrogen atoms toward those particular α protons.

Synthesis of Zirconium Complexes of ^{CY5}[NPN]^{DMP}H$_2$ (2a) and ^{CY5}[NPN]^{DIPP}H$_2$ (2b). The bis(dimethylamido)zirconium(IV) complexes ^{CY5}[NPN]^{DMP}Zr(NMe$_2$)$_2$ (**2a**) and ^{CY5}[NPN]^{DIPP}-Zr(NMe$_2$)$_2$ (**2b**) were obtained starting from Zr(NMe$_2$)$_4$ and the isolated proligands **1** via a protonolysis process. In the case of **2a**, complete conversion is observed after a toluene solution of the reactants is kept at 60 °C for 12 h, while prolonged heating for 2 weeks at 100 °C is required to form the sterically more congested analogue **2b** (see Scheme 3).

The bis(dimethylamido) complexes **2** are obtained as yellow powders in high yields upon workup. For protonolysis to proceed, the tautomeric equilibrium shown in Scheme 2 must be partly operative because this would facilitate the formation of the dienamido complexes **2** from Zr(NMe$_2$)$_4$ by elimination of HNMe$_2$. This is supported by the fact that clean conversions to complexes **2** are observed when the proligands **1** are used as a mixture of isomers.

The ^{31}P{^{1}H} NMR spectra of **2a** and **2b** in C$_6$D$_6$ show singlets at δ −38.9 and −35.5, respectively. Two singlets for the ArCH$_3$ substituents (**2a**) and four doublets for the Ar[CH(CH$_3$)$_2$]$_2$ methyl groups (**2b**) are observed in the ^{1}H{^{31}P} NMR spectrum, indicating that rotation of the *N*-aryl groups is hindered once the ligands are coordinated to zirconium. The dimethylamido ligands are inequivalent as well, which indicates that both complexes have C_s symmetry in solution.

These findings are consistent with the solid-state structures of **2** determined by single-crystal X-ray diffraction. The molecular structure of **2a** is shown in Figure 3 (**2b** is given in Figure S4 in the Supporting Information). Similar to the previously reported [NPN]*Zr(NMe$_2$)$_2$ species (where [NPN]* = {[*N*-(2,4,6-Me$_3$C$_6$H$_2$)(2-*N*-5-MeC$_6$H$_3$)]$_2$PPh}),[4] a distorted trigonal-bipyramidal geometry is found, with the [NPN] ligand coordinating in a facial fashion. The phosphorus donor and one of the dimethylamides in **2a** and **2b** occupy the apical positions, while the remaining amides form the equatorial plane. The observed distortion is mainly due to the acute bite angles of the ligands, which deviate significantly from 90° [**2a**, N1−Zr1−P1 = 73.78(3)°, N2−Zr1−P1 = 72.59(3)°; **2b**, N1−Zr1−P1 = 72.26(6)°, N2−Zr1−P1 = 71.84(6)°]. All nitrogen donors are planar (sp^2-hybridized) and the phosphorus donors pyramidal, with the Zr−N and Zr−P bond

dx.doi.org/10.1021/ic201762r |*Inorg. Chem.* 2011, 50, 11212–11221

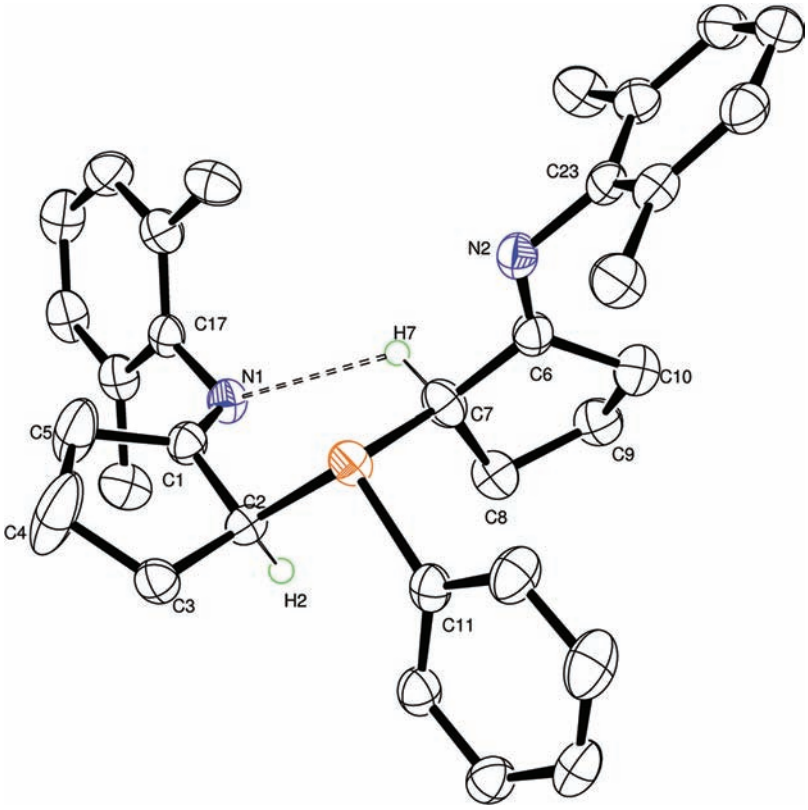

Figure 2. ORTEP drawing of the solid-state molecular structure of the (*SrR*)-*meso*-diimine form of **1a** shown with 50% thermal ellipsoids. The hydrogen atoms have been excluded for clarity except for H2 and H7, whose positions were determined from the difference map. Selected bond lengths (Å) and bond angles (deg): N1−C1 1.2767(4), C1−C2 1.5074(3), C2−P1 1.8509(7), P1−C11 1.8399(4), P1−C7 1.8535(5), C7−C6 1.4887(5), C6−N2 1.2731(4), N1−C17 1.4248(3), N1···H7 2.55(3); C17−N1−C1 119.34(2), N1−C1−C2 122.7(2), C2−P1−C7 102.52(13), P1−C7−C6 114.16(19), C7−C6−N2 122.9(3), C6−N2−C23 121.3(2).

Scheme 3

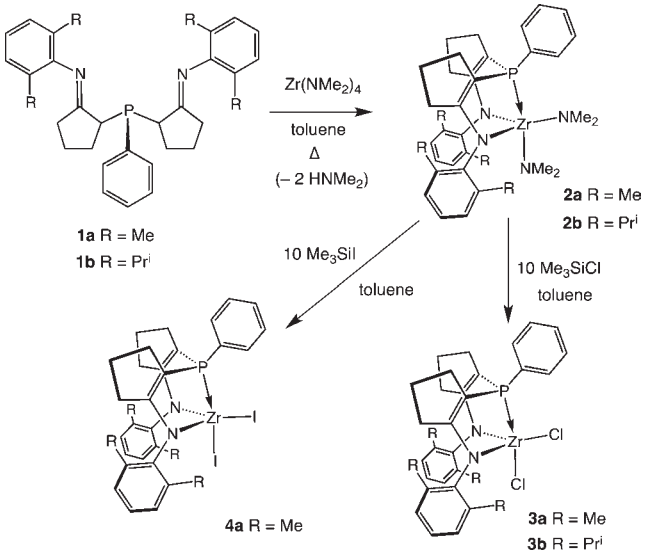

lengths within the values reported for other zirconium(IV) complexes.[45,46]

Starting from the bis(dimethylamido) complexes **2**, the dihalides ^{CY5}[NPN]^{DMP}ZrCl$_2$ (**3a**), ^{CY5}[NPN]^{DIPP}ZrCl$_2$ (**3b**), and ^{CY5}[NPN]^{DMP}ZrI$_2$ (**4a**) are obtained by reaction with excess Me$_3$SiCl or Me$_3$SiI (see Scheme 2). Upon workup, the volatile byproduct Me$_3$SiNMe$_2$ is removed from the reaction mixture under vacuum and the products are isolated as orange powders. Compounds **3** and **4** were fully characterized by NMR spectroscopy, EI-MS, EA, and single-crystal X-ray diffraction.

Dissolution of **3a** and **4a** in tetrahydrofuran (THF) results in a sharp color change from orange to deep red, suggesting that THF adducts are formed. Compared to samples in C_6D_6, the phosphorus resonances in THF-d_8 are shifted downfield from δ −31.9 and −30.1 to δ −21.4 and −23.6 for **3a** and **4a**, respectively. Interestingly, no change in the $^{31}P\{^1H\}$ NMR spectrum is observed when THF is added to **3b**, which indicates that the bulkier *N*-arylisopropyl substituents prevent coordination of THF. As in the case of complexes **2**, hindered rotation around the *N*-aryl bonds is suggested by the observation of inequivalent ^{1}H NMR signals for the *o*-methyl and *o*-isopropyl groups. Combining all of the collected NMR data, an overall C_s symmetry is deduced for **3a**, **3b**, and **4a**.

The ORTEP representations of the solid-state molecular structures of **3a** and **4a** are shown in Figures 4 and 5, respectively (the structure of **3b** can be found in the Supporting Information). In all cases, the geometry around the metal center is best described as distorted trigonal bipyramidal. Similar to the bis(dimethylamido) complexes **2**, the ^{CY5}[NPN] ligands are bound facially with the N−Zr−P angles deviating significantly from 90° due to the strain imposed by the cyclopentenyl linkers. Compared to the previously reported[4] zirconium

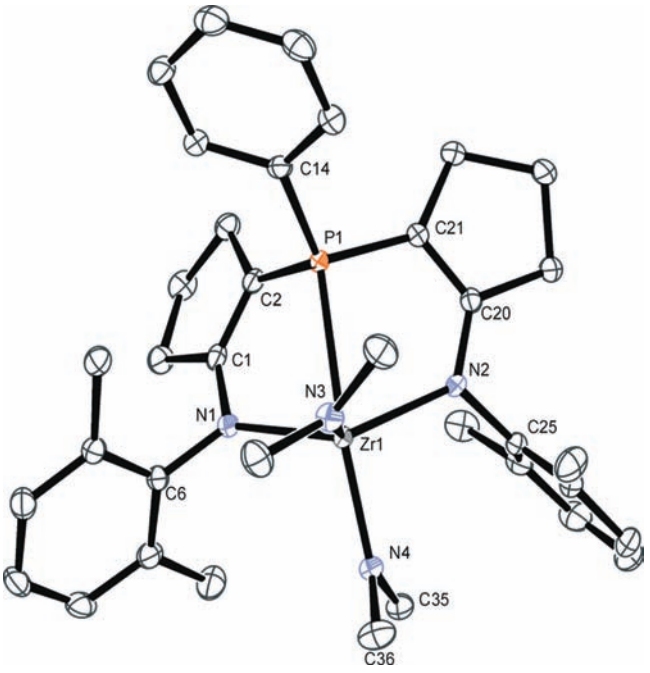

Figure 3. ORTEP drawing of the solid-state molecular structure of **2a** (ellipsoids at the 50% probability level). All hydrogen atoms have been omitted for clarity. Selected bond lengths (Å) and angles (deg): Zr1−N1 2.1727(10), Zr1−N2 2.1740(10), Zr1−P1 2.7756(3), Zr1−N3 2.0191(10), Zr1−N4 2.0670(10), C1−C2 1.3618(16), C20−C21 1.3570(16); N1−Zr1−N2 123.52(4), N3−Zr1−N4 104.88(4), N1−Zr1−P1 73.78(3), N2−Zr1−P1 72.59(3), N1−Zr1−N3 111.36(4), P1−Zr1−N3 89.90(3), P1−Zr1−N4 164.75(3), N1−Zr1−N4 103.49(4), N2−Zr1−N4 97.75(4), N2−Zr1−N3 112.54(4), C2−C1−N1 126.20(10), C21−C20−N2 125.67(10), C6−N1−Zr1 124.83(7), C25−N2−Zr1 118.89(7).

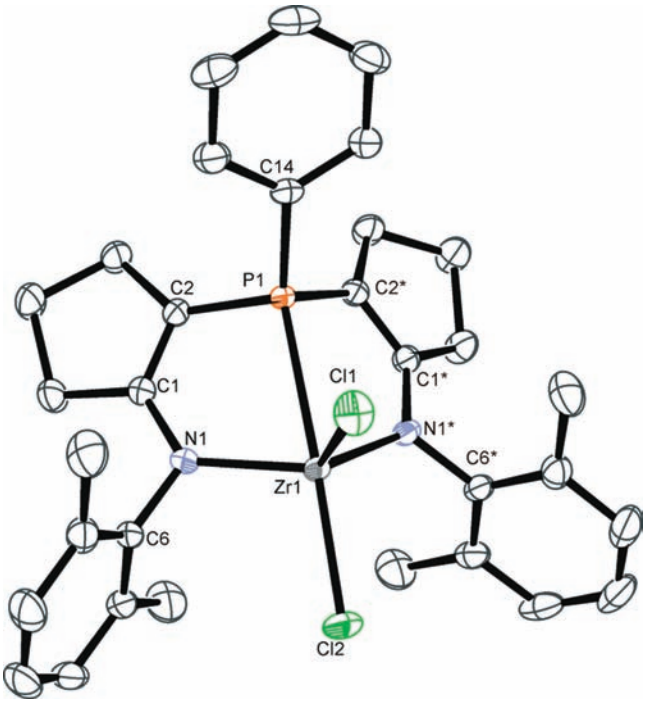

Figure 4. ORTEP drawing of the solid-state molecular structure of **3a** (ellipsoids at the 50% probability level). All hydrogen atoms have been omitted for clarity. Selected bond lengths (Å) and angles (deg): Zr1−N1 2.0844(11), Zr1−P1 2.7689(8), Zr1−Cl1 2.3887(10), Zr1−Cl2 2.4088(8), C1−C2 1.3512(16); N1−Zr1−N1* 120.12(6), Cl1−Zr1−Cl2 100.771(19), N1−Zr1−P1 73.22(3), N1−Zr1−Cl1 112.84(3), P1−Zr1−Cl1 86.401(16), P1−Zr1−Cl2 172.828(18), N1−Z1−Cl2 103.63(3), C2−C1−N1 124.83(11), C6−N1−Zr1 116.55(7).

complex [NPN]*$ZrCl_2$, (where [NPN]* = {[*N*-(2,4,6-$Me_3C_6H_2$)-(2-*N*-5-MeC_6H_3)]$_2$PPh}), the C2−C1−N1 angles in **3** are opened up wider due to geometry imposed by five-membered cyclopentenyl linkers (C2−C1−N1−124° in **4** and ∼118° in [NPN]*$ZrCl_2$).

The structure of **4a** (see Figure 3) closely resembles the structures of **3a** and **3b** with both iodides cis-disposed. The Zr−I bond lengths are 2.79 Å on average, which agrees well with related values reported in the literature.[47]

Synthesis of {^{CY5}[NPN]^{DMP}Zr(THF)}$_2$(μ-η^2:η^2-N_2) (5). We have previously reported that dinuclear side-on-bridging dinitrogen complexes of zirconium can be obtained via KC_8 reduction of a variety of amidophosphine-containing precursor complexes.[26,48−52] For example, reduction of [NPN]*$ZrCl_2$ in THF under 4 atm of N_2 at low temperature in THF leads to the formation of {[NPN]*Zr(THF)}$_2$(μ-η^2:η^2-N_2).[26] When the same methodology was applied, attempts were made to reduce **3a**, **3b**, and **4a** in the presence of molecular nitrogen. In each case, deep-green solutions were initially observed, which decomposed rapidly upon removal of THF. Analysis of the crude reaction mixtures by ^{31}P NMR revealed that multiple products formed and that all starting materials had been consumed. In attempts to separate the different species by fractional crystallization, pentane was added to the crude reaction mixtures (after removal of graphite by filtration over Celite), which resulted in the precipitation of blue solids. These solids were found to be insoluble in all common organic solvents and resisted appropriate characterization. On the basis of the assumption that the latter solids are decomposition products generated by decoordination of THF, we decided to focus our efforts on the reduction of **4a**, which was shown to form a stable THF adduct (vide supra). Thus, **4a** was reacted with 2.2 equiv of KC_8 in THF at −116 °C under 1 atm of N_2 and the reaction mixture slowly warmed to room temperature (see eq 2).

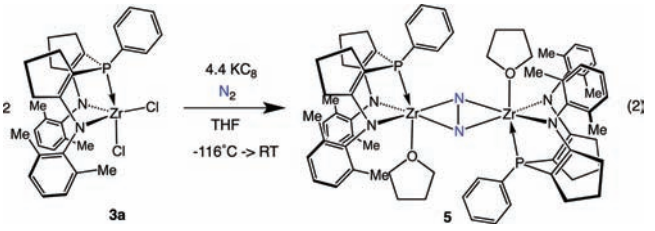

After filtration, slow evaporation of the crude reaction mixture in a glovebox at room temperature generated black crystals over the course of several days, which were analyzed by single-crystal X-ray diffraction. The refined molecular structure revealed that the dinuclear side-on dinitrogen complex **5** formed with one THF molecule coordinated to each metal center (see Figure 6). The Zr_2N_2 unit in this arrangement is almost planar, with a dihedral angle of 179.5° between the two ZrN_2 planes (see Figure 5).

Similar to the N−N bond distance of 1.503(6) Å in {[NPN]*Zr(THF)}$_2$(μ-η^2:η^2-N_2),[26] the N−N bond in **5** is elongated to 1.508(5) Å, corresponding to the hydrazido moiety (N_2^{4-}). This compares well to many of the side-on-bound dinitrogen complexes reported in the literature, as shown in

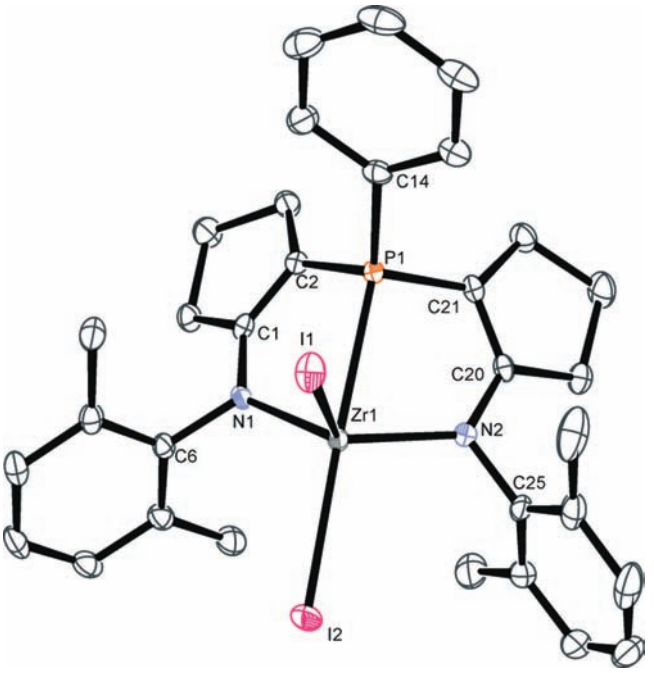

Figure 5. ORTEP drawing of the solid-state molecular structure of **4a** (ellipsoids at 50% probability level). All hydrogen atoms have been omitted for clarity. Selected bond length (Å) and angles (°): Zr1−N1 2.0837(19), Zr1−N2 2.0810(19), Zr1−P1 2.7536(8), Zr1−I1 2.7859(17), Zr1−I2 2.7966(6), C1−C2 1.348(3), C20−C21 1.352(3), N1−Zr1−N2 120.44(8), I1−Zr1−I2 99.59(2), N1−Zr1−P1 72.94(5), N2−Zr1−P1 72.96(5), N1−Zr1−I1 109.59(6), P1−Zr1−I1 84.54(3), P1−Zr1−I2 175.773(16), N1−Zr1−I2 106.29(5), N2−Zr1−I2 104.31(5), N2−Zr1−I1 113.98(6), C6−N1−Zr1 117.04(14), C25−N2−Zr1 117.44(14), C2−C1−N1 124.6(2), C21−C20−N2 124.2(2).

Table 1.[26,48−55] With respect to **5**, a 2-fold rotation axis bisects the N−N bond perpendicular to the Zr_2N_2 plane, resulting in an overall C_2 symmetry (Figure 7). The Zr−N bond lengths of the N_2 core are slightly different from each other [Zr1−N3 = 2.017(3) Å and Zr1−N3* = 2.073(3) Å] and significantly shorter than the Zr−N(ligand) bonds [Zr1−N1 = 2.237(3) Å and Zr1−N2 = 2.189(3) Å]; the Zr1−P1 [2.7136(9) Å] and Zr1−O1 [2.348(2) Å] bond lengths are unexceptional.

Despite several efforts, well-resolved NMR spectra of **5** in THF-d_8 or C_6D_6 were not obtained. Upon isolation of the black crystals from a THF solution, rapid decomposition to the already mentioned blue solids is observed, which prevented the acquisition of other spectroscopic and analytical data.

CONCLUSIONS

In this paper, two new diiminophosphine proligands **1** and their zirconium complexes **2**−**4** were prepared and fully characterized. The proligands exist as a mixture of isomers because of the presence of tautomers and stereoisomers. Nevertheless, the various isomers of both **1a** and **1b** are cleanly deprotonated upon reaction with $Zr(NMe_2)_4$ to form the dienamido compounds **2a** and **2b**, respectively. The potential of the new zirconium NPN complexes **3** and **4** to activate dinitrogen upon reduction was explored and the THF-solvated side-on dinitrogen complex **5** obtained. The latter compound is unstable, presumably because of desolvation, which prevented full characterization as well as reactivity studies. Attempts to reduce complex **3b**, which incorporates the bulkier DIPP-substituted ligand, did not produce any isolable dinitrogen-containing products.

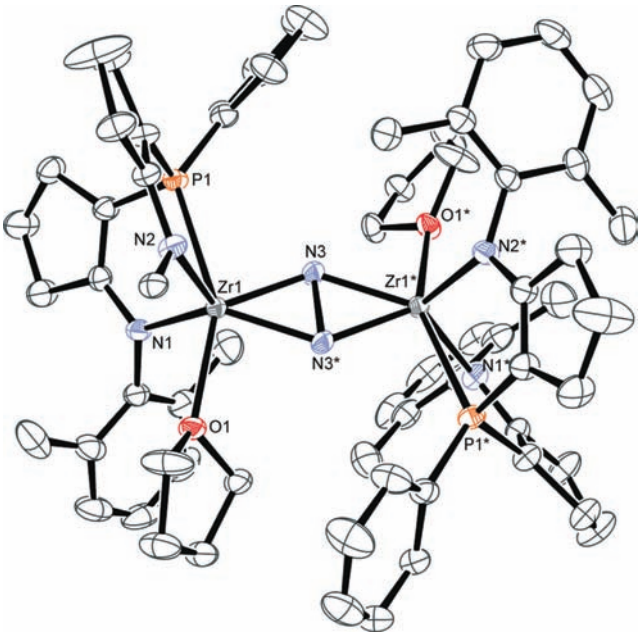

Figure 6. ORTEP drawing of the solid-state molecular structure of **5** (ellipsoids at the 50% probability level). All hydrogen atoms have been omitted for clarity. Carbons of one of the 2,6-dimethylphenyl substituents (except C_{ipso}) on the N2 donor are omitted for clarity. Selected bond lengths (Å) and angles (deg): Zr1−P1 2.7136(9), Zr1−N1 2.237(3), Zr1−N2 2.189(3), Zr1−O1 2.348(2), Zr1−N3 2.017(3), Zr1−N3* 2.073(3), N3−N3* 1.508(5); P1−Zr1−N1 74.35(7), P1−Zr1−N2 74.61(7), N3−Zr1−N3* 43.25(14), Zr1−N3−Zr1* 136.75(14), O1−Zr1−P1 152.32(6), P1−Zr1−N3 82.54(8).

Table 1. Selected Dinuclear Zirconium Dinitrogen Complexes with Side-On-Bound Dinitrogen

compound	N−N bond length (Å)
$([PNP]ZrCl)_2(\mu\text{-}\eta^2\text{:}\eta^2\text{-}N_2)^a$	1.587(7)[49]
$([PNP]Zr(O\text{-}2,6\text{-}Me_2C_6H_3))_2(\mu\text{-}\eta^2\text{:}\eta^2\text{-}N_2)$	1.528(7)[48]
$([P_2N_2]Zr)_2(\mu\text{-}\eta^2\text{:}\eta^2\text{-}N_2)^b$	1.465(19)[51]
$\{[NPN]Zr(THF)\}_2(\mu\text{-}\eta^2\text{:}\eta^2\text{-}N_2)^c$	1.503(3)[52]
$\{[NPN]^*Zr(THF)\}_2(\mu\text{-}\eta^2\text{:}\eta^2\text{-}N_2)^d$	1.503(6)[26]
$[\eta^5\text{-}C_5Me_4H)_2Zr]_2(\mu\text{-}\eta^2\text{:}\eta^2\text{-}N_2)$	1.377(3)[55]
$(rac\text{-}BpZr)_2(\mu\text{-}\eta^2\text{:}\eta^2\text{-}N_2)^e$	1.241(2)[53]
$[Cp''_2Zr]_2(\mu\text{-}\eta^2\text{:}\eta^2\text{-}N_2)^f$	1.47(3)[54]
$((\eta^5\text{-}C_5Me_5)Zr(^tPrNC(NMe_2)N^iPr))_2(\mu\text{-}\eta^2\text{:}\eta^2\text{-}N_2)$	1.518(2)[50]
$\{^{CYS}[NPN]^{DMP}Zr(THF)\}_2(\mu\text{-}\eta^2\text{:}\eta^2\text{-}N_2)^g$	1.508(5)

[a] [PNP] = $N(SiMe_2CH_2PPr^i_2)_2$. [b] [P_2N_2 = $PhP(CH_2SiMe_2NSiMe_2CH_2)_2PPh$. [c] [NPN] = $PhP(CH_2SiMe_2NPh)_2$. [d] [NPN]* = {[*N*-(2,4,6-$Me_3C_6H_2$)(2-*N*-5-MeC_6H_3)]$_2$PPh}. [e] *rac*-Bp = *rac*-$Me_2Si(\eta^5\text{-}C_5H_2\text{-}2\text{-}SiMe_3\text{-}4\text{-}CMe_3)_2$. [f] Cp″ = η^5-1,3-$C_5H_3(SiMe_3)_2$. [g] **5** (Figure 6).

EXPERIMENTAL SECTION

General Considerations. Unless otherwise stated, all manipulations were performed under an atmosphere of dry, oxygen-free N_2 or Ar by means of standard Schlenk or glovebox techniques. Hexanes, toluene, THF, and diethyl ether were purchased anhydrous from Aldrich, sparged

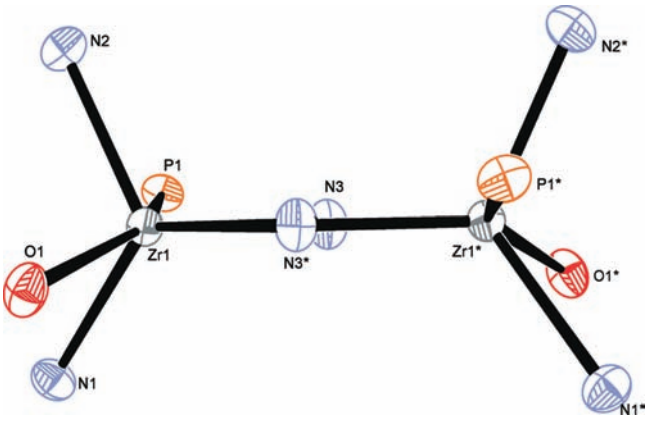

Figure 7. Side view of the stereochemistry around the $Zr_2(\eta^2{:}\eta^2\text{-}N_2)$ core in **5**.

with N_2, and passed through columns containing activated alumina and Ridox catalyst. C_6D_6 was dried by distillation from sodium/benzophenone onto activated 4 Å molecular sieves and freeze−pump−thaw degassed three times. Pentane and benzene were dried over sodium/benzophenone and distilled prior to use. Unless otherwise noted, ^{1}H, $^{31}P\{^1H\}$, and $^{13}C\{^1H\}$ NMR spectra were recorded on a Bruker AV-300 or a Bruker AV-400 spectrometer, operating at 300.1 and 400.0 MHz for ^{1}H NMR spectra, respectively. All spectra were recorded at room temperature. ^{1}H NMR spectra were referenced to residual protons in the deuterated solvent C_6D_6 (δ 7.16). $^{31}P\{^1H\}$ NMR spectra were referenced to external $P(OMe)_3$ (δ 141.0 with respect to 85% H_3PO_4 at δ 0.0). $^{13}C\{^1H\}$ NMR spectra were referenced to the residual solvent C_6D_6 (δ 128.0). Chemical shifts (δ) listed are in parts per million, and absolute values of the coupling constants are in hertz. EI-MS, EA (C, H, and N), and X-ray crystallography were all performed at the Department of Chemistry, University of British Columbia.

Dichlorophenylphosphine was purified by distillation. Diisopropylamine was dried over CaH_2 and distilled prior to use. *n*-Butyllithium was purchased from Aldrich, and the molarity was determined via direct titration with diphenylcarboxylic acid.[56] KC_8 was prepared according to a literature procedure.[57] All other compounds were purchased from commercial suppliers and used as received.

Synthesis of 1a. In a round-bottomed flask, LDA was prepared by the slow addition of 1.63 M *n*-butyllithium (8.72 mL, 14.2 mmol) to diisopropylamine (2.00 mL, 14.2 mmol) in 20 mL of diethyl ether at −78 °C. The resulting mixture was stirred for 30 min during warming to −50 °C. The solution was cooled to −78 °C again, and neat *N*-cyclopentylidene-2,6-dimethylaniline (2.66 g, 14.2 mmol) was added dropwise. Thereafter, the reaction mixture was warmed to −40 °C over 1 h. Afterward, the mixture was cooled again to −78 °C, and a solution of dichlorophenylphosphine (0.96 mL, 7.10 mmol) in 80 mL of diethyl ether was added over 1 h. The colorless solution gradually changed to pale yellow. Upon completion, the reaction vessel was warmed to room temperature and stirred overnight. The volatiles were then removed in vacuo, and 20 mL of toluene was added to the mixture, which was filtered through Celite using a glass frit. Toluene was removed in vacuo, giving a yellow oil consisting of a mixture of isomers ($^{31}P\{^1H\}$ NMR signals at δ −5.6, −6.0, −8.5, −12.1, −32.1, and −36.7 in toluene). To the mixture was added 10 mL of pentane to generate a white precipitate. The suspension was cooled to −40 °C overnight, and the solid was collected on a glass frit and dried in vacuo. Yield: 1.62 g, 41%.

^{1}H NMR (C_6D_6, 600 MHz). Several structural and stereoisomers exist in various amounts. The number of protons is based on integration of each of these resonances relative to the α protons of the *meso*-diimine tautomer at δ 3.86 (t, 2H, 8 Hz): δ 8.12 (t, 0.53H, *o*-PPh), 7.99 (t, 0.21H, 7 Hz, *o*-PPh), 7.85 (dd, 1.15H, 4.25 and 10.25 Hz, *o*-PPh), 7.72 (m, 2.42H, *o*-PPh), 6.87−7.29 (m, 20H, *m*-NAr and *o*-NAr), 6.47 (d, 0.12H, 4 Hz, N−H), 6.11 (d, 0.27H, 6 Hz, N−H), 4.62 (t, 0.58H, 7 Hz, α-CH *rac*), 4.21 (t, 0.58H, 9 Hz, α-CH *rac*), 3.89 (t, 2H, 8 Hz, α-CH *meso*), 3.73 (t, 0.41H, 8 Hz, α-CH enamineimine), 3.64 (dd, 0.31H, 6 and 10 Hz, α-CH enamineimine), 2.28 (s, 0.72H, $ArCH_3$), 2.26 (s, 2H, $ArCH_3$), 2.17 (s, 6H, $ArCH_3$), 2.15 (s, 2H, $ArCH_3$), 2.14 (s, 1H, $ArCH_3$), 2.12 (s, 3H, $ArCH_3$), 2.09 (s, 2H, $ArCH_3$), 2.08 (s, 1H, $ArCH_3$), 2.07 (s, 6H, $ArCH_3$), 1.88−2.06 (m, 7H, CH_2), 1.85 (s, 2H, $ArCH_3$), 1.19−1.83 (m, 22H, CH_2).

*^{1}H NMR of Pure meso-**1a** (C_6D_6, 300 MHz):* δ 7.74 (m, 2H, *o*-PPh), 7.18 (m, 3H, *m*- and *p*-PPh), 7.05 (d, 4H, 6 Hz, *m*-NAr), 6.94 (t, 2H, 6 Hz, *p*-NAr), 3.88 (t, 2H, 6 Hz, CH), 2.19 (s, 6H, $ArCH_3$), 2.09 (s, 6H, $ArCH_3$), 2.05 (m, 2H, CH_2), 1.68 (m, 6H, CH_2), 1.45 (m, 2H, CH_2), 1.30 (m, 2H, CH_2). $^{31}P\{^1H\}$ NMR (C_6D_6, 161 MHz): δ −9.4 (s). $^{13}C\{^1H\}$ NMR (C_6D_6, 101 MHz): δ 181.2 (d, 9 Hz), 151.0, 135.7, 135.6 (d, 36 Hz), 129.3, 128.5, 128.3, 128.1, 127.8, 125.5 (d, 23 Hz), 122.9, 42.4 (d, 19 Hz), 32.6, 28.4 (d, 6 Hz), 23.6 (d, 5 Hz), 18.9, 18.3 ($ArCH_3$). EI-MS (*m*/*z*): 480 ($[M]^+$). Anal. Calcd for $C_{32}H_{37}N_2P$: C, 79.97; H, 7.76; N, 5.83. Found: C, 80.06; H, 7.88; N, 5.70.

Synthesis of 1b. In a round-bottomed flask, LDA was prepared by the slow addition of 1.6 M *n*-butyllithium (7.04 mL, 11.5 mmol) to diisopropylamine (1.62 mL, 11.5 mmol) in 20 mL of diethyl ether at −78 °C. The resulting mixture was stirred for 30 min during warming to −50 °C. The solution was cooled to −78 °C again, and neat *N*-cyclopentylidene-2,6-diisopropylaniline (2.81 g, 11.5 mmol) was added dropwise. Thereafter, the reaction mixture was warmed to −40 °C over 1 h. The mixture was cooled to −78 °C again, and a solution of dichlorophenylphosphine (0.78 mL, 5.75 mmol) in 80 mL of diethyl ether was added over 1 h. The colorless solution gradually changed to pale yellow. Upon completion, the reaction vessel was warmed to room temperature and stirred overnight. The volatiles were then removed in vacuo, and 20 mL of toluene was added to the mixture, which was filtered through Celite using a glass frit. Toluene was removed in vacuo to give a yellow oil, which consists of a mixture of isomers ($^{31}P\{^1H\}$ NMR signals at δ −2.9, −3.8, −8.8, −28.5, and −37.2 in toluene). A total of 10 mL of pentane was added to the residue, which resulted in the formation of a white precipitate. The suspension was cooled to −40 °C overnight, and the precipitate was collected on a glass frit and dried in vacuo. Yield: 1.64 g, 48%. ^{1}H NMR (C_6D_6, 400 MHz): δ 7.71 (dd, 2H, J_{HP} = 8 Hz, J_{HH} = 8 Hz, *o*-PPh), 7.19−7.09 (m, overlap with the solvent peak), 3.83 (t, 2H, 8 Hz, CH), 3.05 (sept, 4H, 4 Hz, CH), 2.10 (m, 2H, CH_2), 1.89 (m, 2H, CH_2), 1.70 (m, 4H, CH_2), 1.46 (m, 2H, CH_2), 1.35 (m, 2H, CH_2), 1.29 (d, 6H, 4 Hz, CH_3), 1.24 (d, 6H, 4 Hz, CH_3), 1.16 (d, 6H, 4 Hz, CH_3), 1.15 (d, 6H, 4 Hz, CH_3). $^{31}P\{^1H\}$ NMR (C_6D_6, 161 MHz): δ −8.8 (s). $^{13}C\{^1H\}$ NMR (C_6D_6, 75 MHz): δ 181.3 (d, 8 Hz), 148.2, 136.2, 136.0, 135.8, 135.6, 135.4 (d, 26 Hz), 129.3, 128.0, 123.5 (d, 25 Hz), 123.2, 42.8 (d, 20 Hz), 33.0, 28.4, 28.2 (d, 6 Hz), 27.8, 24.6, 23.7 (d, 5 Hz), 23.4, 23.1, 22.9. EI-MS (*m*/*z*): 592 ($[M]^+$), 549 ($[M - CH(CH_3)_2]^+$). Anal. Calcd for $C_{40}H_{53}N_2P$: C, 81.04; H, 9.01; N, 4.73. Found: C, 81.16; H, 8.86; N, 4.85.

Synthesis of 2a. $Zr(NMe_2)_4$ (1.463 g, 3.05 mmol) and **1a** (0.815 g, 3.05 mmol) were combined and dissolved in toluene (20 mL). The reaction mixture was then transferred to a 100-mL Kontes-sealed reaction vessel (bomb) and stirred in an oil bath at 60 °C for 12 h. The resulting yellow solution was taken to dryness to obtain a yellow residue. Upon the addition of pentane (10 mL), a light-yellow precipitate formed and was collected on a frit and dried (1.71 g, 2.60 mmol, 85%). Yellow single crystals of **2a** suitable for X-ray diffraction were grown by the slow evaporation of a pentane solution of the compound.

^{1}H NMR (C_6D_6, 400 MHz): δ 7.58 (dd, 2H, J_{HP} = 8 Hz, J_{HH} = 8 Hz, *o*-PPh), 7.25 (t, 2H, 8 Hz, *m*-PPh), 7.11 (t, 1H, 8 Hz, *p*-PPh), 7.05 (d, 2H, 8 Hz, *m*-NAr), 7.03 (d, 2H, 8 Hz, *m*-NAr), 6.92 (t, 2H, 8 Hz, *p*-NAr), 2.90 (s, 6H, $N(CH_3)_2$), 2.74 (m, 2H), 2.53 (m, 2H), 2.34 (s, 6H, $ArCH_3$), 2.33 (s, 6H, $ArCH_3$), 2.24 (s, 6H, $N(CH_3)_2$), 2.08 (m, 2H),

dx.doi.org/10.1021/ic201762r |*Inorg. Chem.* 2011, 50, 11212–11221

1.90 (m, 6H). $^{31}P\{^1H\}$ NMR (C_6D_6, 162 MHz): δ −38.9 (s). $^{13}C\{^1H\}$ NMR (C_6D_6, 101 MHz): δ 173.1 (d, 37 Hz), 148.9, 135.7, 134.7, 133.9 (d, 32 Hz), 131.2 (d, 12 Hz), 128.7, 128.6, 128.1, 127.8, 124.3, 93.5 (d, 32 Hz), 42.8, 42.2, 34.2 (d, 11 Hz), 31.0 (d, 3 Hz), 24.3 (d, 6 Hz), 19.5, 19.4. EI-MS (m/z): 656 ($[M]^+$), 612 ($[M - NMe_2]^+$). Anal. Calcd for $C_{36}H_{47}N_4PZr$: C, 65.71; H, 7.20; N, 8.51. Found: C, 65.36; H, 7.30; N, 8.24.

Synthesis of 3a. To a stirred yellow toluene solution (30 mL) of **2a** (1.53 g, 2.33 mmol) was added chlorotrimethylsilane (2.53 g, 23.3 mmol) dropwise. The solution was stirred overnight. An orange precipitate gradually formed. The reaction mixture was taken to dryness to obtain an orange powder, which was collected on a frit, washed with pentane (3 × 5 mL), and dried (1.42 g, 2.22 mmol, 95%). X-ray-quality orange crystals of **3a** were grown by the slow evaporation of a benzene solution of the compound.

^1H NMR (C_6D_6, 400 MHz): δ 7.58 (dd, 2H, J_{HP} = 8 Hz, J_{HH} = 8 Hz, *o*-PPh), 7.16 (t, 2H, 8 Hz, *m*-PPh), 7.06 (t, 1H, 8 Hz, *p*-PPh), 6.96 (m, 6H), 2.64 (m, 2H), 2.48 (s, 6H, $ArCH_3$), 2.50 (m, 2H), 2.43 (s, 6H, $ArCH_3$), 1.91 (m, 2H), 1.78 (m, 2H), 1.69 (m, 4H). $^{31}P\{^1H\}$ NMR (C_6D_6, 162 MHz): δ −31.9 (s). $^{13}C\{^1H\}$ NMR (C_6D_6, 101 MHz): δ 172.4 (d, 51 Hz), 143.5, 135.8 (d, 35 Hz), 130.7 (d, 15 Hz), 129.7, 129.4, 129.2, 129.1, 128.7, 128.4, 127.4, 103.6 (d, 53 Hz), 32.5 (d, 18 Hz), 30.6 (d, 5 Hz), 24.0 (d, 9 Hz), 19.7, 19.0. EI-MS (m/z): 640 ($[M]^+$), 532 ($[M - PPh]^+$). Anal. Calcd for $C_{32}H_{35}Cl_2N_2PZr \cdot 0.73$ toluene: C, 62.93; H, 5.82; N, 3.96. Found: C, 62.58; H, 5.79; N, 3.88.

Synthesis of 4a. To a stirred yellow toluene solution (5 mL) of **2a** (0.276 g, 0.421 mmol) was added trimethylsilane iodide (0.842 g, 4.21 mmol) dropwise. The solution was stirred overnight. An orange precipitate gradually formed. The reaction mixture was taken to dryness to give a deep-orange powder, which was collected on a frit, washed with pentane (3 × 1 mL), and dried (0.318 g, 0.387 mmol, 92%). X-ray-quality crystals of **4a** were grown by the slow diffusion of pentane into a benzene solution of the compound.

^1H NMR (C_6D_6, 400 MHz): δ 7.49 (dd, 2H, J_{HP} = 8 Hz, J_{HH} = 8 Hz, *o*-PPh), 7.18 (t, 2H, 8 Hz, *m*-PPh), 7.07 (t, 1H, 8 Hz, *p*-PPh), 7.05 (t, 2H, 8 Hz, *p*-NAr), 6.98 (m, 4H, *m*-NAr), 2.63 (s, 6H, $ArCH_3$), 2.58 (m, 2H), 2.39 (m, 2H), 2.36 (s, 6H), 1.92 (m, 2H), 1.74 (m, 6H). $^{31}P\{^1H\}$ NMR (C_6D_6, 162 MHz): δ −30.1 (s). $^{13}C\{^1H\}$ NMR (C_6D_6, 101 MHz): δ 172.8 (d, 36 Hz), 142.8, 136.2 (d, 30 Hz), 130.6 (d, 10 Hz), 129.8, 129.7, 129.2, 129.1, 129.0, 128.0, 127.8, 105.7 (d, 38 Hz), 32.9 (d, 12 Hz), 31.1 (d, 3 Hz), 24.30 (d, 6 Hz), 21.1, 20.8. EI-MS (m/z): 822 ($[M]^+$), 695 ($[M - I]^+$). Anal. Calcd for $C_{32}H_{35}I_2N_2PZr$: C, 46.66; H, 4.28; N, 3.40. Found: C, 46.64; H, 4.58; N, 3.27.

Synthesis of 2b. $Zr(NMe_2)_4$ (0.186 g, 0.699 mmol) and **1b** (0.414 g, 0.699 mmol) were mixed together and dissolved in toluene (10 mL). The reaction mixture was then transferred to a 100-mL Kontes-sealed reaction vessel (bomb) and stirred in an oil bath at 100 °C for 10 days. The resulting yellow solution was taken to dryness to obtain a yellow residue. Upon the addition of pentane (5 mL), a light-yellow precipitate formed and was collected on a frit and dried (0.435 g, 0.566 mmol, 81%). Yellow single crystals of **2b** suitable for X-ray diffraction were grown by the slow evaporation of a pentane solution of the compound.

^1H NMR (C_6D_6, 400 MHz): δ 7.58 (dd, 2H, J_{HP} = 8 Hz, J_{HH} = 8 Hz, *o*-PPh), 7.28 (t, 2H, 8 Hz, *m*-PPh), 7.18 (t, 2H, 8 Hz, *p*-NAr), 7.16 (t, 2H, 8 Hz, *p*-PPh), 7.10 (m, 4H, *m*-NAr), 3.60 (sept, 4H, 4 Hz, CH), 2.71 (s, 6H, $N(CH_3)_2$), 2.70 (m, 2H), 2.51 (s, 6H, $N(CH_3)_2$), 2.49 (m, 2H), 2.17 (m, 4H, CH_2), 1.88 (m, 2H, CH_2), 1.76 (m, 2H, CH_2), 1.32 (d, 6H, 4 Hz, CCH_3), 1.30 (d, 6H, 4 Hz, CCH_3), 1.21 (d, 6H, 4 Hz, CCH_3), 1.10 (d, 6H, 4 Hz, CCH_3). $^{31}P\{^1H\}$ NMR (C_6D_6, 162 MHz): δ −35.5 (s). $^{13}C\{^1H\}$ NMR (C_6D_6, 101 MHz): δ 173.9 (d, 33 Hz), 146.3, 144.9, 134.2, 131.4 (d, 13), 128.6 (d, 9 Hz), 128.1, 127.8, 125.3, 123.8, 123.4, 90.6 (d, 35), 42.3, 40.5, 34.8 (d, 9 Hz), 31.3 (d, 3 Hz), 27.9, 27.7, 25.7, 25.2, 24.6 (d, 5 Hz), 23.7. EI-MS (m/z): 768 ($[M]^+$), 725 ($[M - CH(CH_3)_2]^+$). Anal. Calcd for $C_{44}H_{63}N_4PZr$: C, 68.62; H, 8.24; N, 7.27. Found: C, 68.37; H, 7.86; N, 6.94.

Synthesis of 3b. To a stirred yellow toluene solution (10 mL) of **2b** (0.601 g, 0.782 mmol) was added trimethylsilane chloride (0.845 g, 7.82 mmol) dropwise. The solution was stirred overnight. An orange precipitate gradually formed. The reaction mixture was taken to dryness to obtain an orange powder, which was collected on a frit, washed with pentane (3 × 2 mL), and dried (0.563 g, 0.751 mmol, 96%). X-ray-quality orange crystals of **3b** were grown by the slow evaporation of a benzene solution of the compound.

^1H NMR (C_6D_6, 300 MHz): δ 7.63 (dd, 2H, J_{HP} = 6 Hz, J_{HH} = 6 Hz, *o*-PPh), 7.19−7.14 (m, overlap with the solvent peak), 7.08 (m, 3H), 3,68 (sept, 2H, 6 Hz, CH), 3.44 (sept, 2H, 6 Hz, CH), 2.60 (m, 2H), 2.49 (m, 2H), 2.14 (m, 2H), 1.78 (m, 4H), 1.64 (m, 2H), 1.53 (d, 6H, 6 Hz, CH_3), 1.42 (d, 6H, 6 Hz, CH_3), 1.19 (d, 6H, 6 Hz, CH_3), 1.09 (d, 6H, 6 Hz, CH_3). $^{31}P\{^1H\}$ NMR (C_6D_6, 121 MHz): δ −32.3 (s). $^{13}C\{^1H\}$ NMR (C_6D_6, 101 MHz): δ 172.3 (d, 48 Hz), 146.3, 145.0, 141.9, 131.2 (d, 16 Hz), 129.9, 128.9 (d, 13 Hz), 128.0, 127.7, 124.9, 124.4, 102.4 (d, 50 Hz), 34.1 (d, 17 Hz), 31.0 (d, 4 Hz), 29.0, 28.5, 25.7, 25.6, 24.4, 24.3 (d, 8 Hz), 24.0. EI-MS (m/z): 752 ($[M]^+$). Anal. Calcd for $C_{40}H_{51}Cl_2N_2PZr$: C, 63.81; H, 6.83; N, 3.72. Found: C, 63.54; H, 6.63; N, 3.72.

General Procedure for the Reduction Reactions. Compound **3a** (0.296 g, 0.463 mmol) and KC_8 (0.137 g, 1.02 mmol) were added to a 200-mL thick-walled Kontes-sealed reaction vessel (bomb) and shaken to mix thoroughly. THF (10 mL) was vacuum-transferred to the solid mixture at −196 °C. The flask was filled with dinitrogen at −196 °C, sealed, and warmed slowly to room temperature in a liquid-dinitrogen/dry ice/EtOH slurry behind a blast shield. After the mixture had gradually melted over 1 h, it was stirred vigorously. The solution was stirred overnight. The next day the bomb was depressurized by first cooling to −196 °C, opening the seal to dinitrogen, and allowing the bomb to warm to room temperature. The green solution was filtered through Celite to remove all of the residual graphite and salt. The filtrate was concentrated to about 3 mL, and pentane (5 mL) was added. Some blue solid quickly precipitated out. Crystals of **6** suitable for X-ray analysis were grown in an NMR tube by the slow evaporation of the THF solution.

■ ASSOCIATED CONTENT

Supporting Information. Crystallographic data in CIF format for **1**−**5** and details on X-ray structure refinement, ORTEP diagrams for **1b**, **2b**, and **3b**, and ^1H NMR and ^{13}C HSQC NMR spectra of the mixture of compounds of **1a**. This material is available free of charge via the Internet at http://pubs.acs.org.

■ AUTHOR INFORMATION

Corresponding Author

*E-mail: fryzuk@chem.ubc.ca.

■ ACKNOWLEDGMENT

We thank NSERC of Canada for funding (Discovery Grant to M.D.F.). We also thank Nathan Halcovitch and Dr. Brian O. Patrick for help with the X-ray structures.

■ REFERENCES

(1) Schrock, R. R.; Seidel, S. W.; Schrodi, Y.; Davis, W. M. *Organometallics* **1999**, *18*, 428.

(2) Wang, W.; Yang, L.; Foxman, B. M.; Ozerov, O. V. *Organometallics* **2004**, *23*, 4700.

(3) Bailey, B. C.; Huffman, J. C.; Mindiola, D. J.; Weng, W.; Ozerov, O. V. *Organometallics* **2005**, *24*, 1390.

(4) MacLachlan, E. A.; Fryzuk, M. D. *Organometallics* **2005**, *24*, 1112.

(5) Lee, J.-H.; Pink, M.; Tomaszewski, J.; Fan, H.; Caulton, K. G. *J. Am. Chem. Soc.* **2007**, *129*, 8706.
(6) Menard, G.; Jong, H.; Fryzuk, M. D. *Organometallics* **2009**, *28*, 5253.
(7) Whited, M. T.; Grubbs, R. H. *Acc. Chem. Res.* **2009**, *42*, 1607.
(8) Brookes, N. J.; Whited, M. T.; Ariafard, A.; Stranger, R.; Grubbs, R. H.; Yates, B. F. *Organometallics* **2010**, *29*, 4239.
(9) Gregor, L. C.; Chen, C.-H.; Fafard, C. M.; Fan, L.; Guo, C.; Foxman, B. M.; Gusev, D. G.; Ozerov, O. V. *Dalton Trans.* **2010**, *39*, 3195.
(10) Fryzuk, M. D.; MacNeil, P. A. *J. Am. Chem. Soc.* **1981**, *103*, 3592.
(11) Fryzuk, M. D.; MacNeil, P. A.; Rettig, S. J.; Secco, A. S.; Trotter, J. *Organometallics* **1982**, *1*, 918.
(12) Fryzuk, M. D.; Giesbrecht, G. R.; Rettig, S. J. *Inorg. Chem.* **1998**, *37*, 6928.
(13) Fryzuk, M. D.; Love, J. B.; Rettig, S. J. *Organometallics* **1998**, *17*, 846.
(14) Fryzuk, M. D.; Giesbrecht, G. R.; Rettig, S. J.; Yap, G. P. A. *J. Organomet. Chem.* **1999**, *591*, 63.
(15) Fryzuk, M. D.; Johnson, S. A.; Rettig, S. J. *Organometallics* **1999**, *18*, 4059.
(16) Fryzuk, M. D.; Jafarpour, L.; Kerton, F. M.; Love, J. B.; Patrick, B. O.; Rettig, S. J. *Organometallics* **2001**, *20*, 1387.
(17) Fryzuk, M. D.; Petrella, M. J.; Coffin, R. C.; Patrick, B. O. *C. R. Chim.* **2002**, *5*, 451.
(18) Fryzuk, M. D.; Shaver, M. P.; Patrick, B. O. *Inorg. Chim. Acta* **2003**, *350*, 293.
(19) Shaver, M. P.; Thomson, R. K.; Patrick, B. O.; Fryzuk, M. D. *Can. J. Chem.* **2003**, *81*, 1431.
(20) Fryzuk, M. D.; Johnson, S. A.; Rettig, S. J. *J. Am. Chem. Soc.* **1998**, *120*, 11024.
(21) Fryzuk, M. D.; Johnson, S. A.; Patrick, B. O.; Albinati, A.; Mason, S. A.; Koetzle, T. F. *J. Am. Chem. Soc.* **2001**, *123*, 3960.
(22) Fryzuk, M. D.; Yu, P.; Patrick, B. O. *Can. J. Chem.* **2001**, *79*, 1194.
(23) Fryzuk, M. D.; MacKay, B. A.; Johnson, S. A.; Patrick, B. O. *Angew. Chem., Int. Ed.* **2002**, *41*, 3709.
(24) Fryzuk, M. D.; MacKay, B. A.; Patrick, B. O. *J. Am. Chem. Soc.* **2003**, *125*, 3234.
(25) Studt, F.; MacKay, B. A.; Fryzuk, M. D.; Tuczek, F. *J. Am. Chem. Soc.* **2004**, *126*, 280.
(26) MacLachlan, E. A.; Hess, F. M.; Patrick, B. O.; Fryzuk, M. D. *J. Am. Chem. Soc.* **2007**, *129*, 10895.
(27) Fryzuk, M. D. *Acc. Chem. Res.* **2009**, *42*, 127.
(28) Ballmann, J.; Yeo, A.; MacKay, B. A.; van Rijt, S.; Patrick, B. O.; Fryzuk, M. D. *Chem. Commun.* **2010**, *46*, 8794.
(29) Ballmann, J.; Yeo, A.; Patrick, B. O.; Fryzuk, M. D. *Angew. Chem., Int. Ed.* **2011**, *50*, 507.
(30) Atienza, C. C. H.; Bowman, A. C.; Lobkovsky, E.; Chirik, P. J. *J. Am. Chem. Soc.* **2010**, *132*, 16343.
(31) Bowman, A. C.; Milsmann, C.; Bill, E.; Lobkovsky, E.; Weyhermuller, T.; Wieghardt, K.; Chirik, P. J. *Inorg. Chem.* **2010**, *49*, 6110.
(32) Enright, D.; Gambarotta, S.; Yap, G. P. A.; Budzelaar, P. H. M. *Angew. Chem., Int. Ed.* **2002**, *41*, 3873.
(33) Korobkov, I.; Gorelsky, S.; Gambarotta, S. *J. Am. Chem. Soc.* **2009**, *131*, 10406.
(34) Russell, S. K.; Darmon, J. M.; Lobkovsky, E.; Chirik, P. J. *Inorg. Chem.* **2010**, *49*, 2782.
(35) Russell, S. K.; Lobkovsky, E.; Chirik, P. J. *J. Am. Chem. Soc.* **2011**, *133*, 8858.
(36) Russell, S. K.; Milsmann, C.; Lobkovsky, E.; Weyhermuller, T.; Chirik, P. J. *Inorg. Chem.* **2011**, *50*, 3159.
(37) Scott, J.; Gambarotta, S.; Korobkov, I.; Budzelaar, P. H. M. *J. Am. Chem. Soc.* **2005**, *127*, 13019.
(38) Tondreau, A. M.; Milsmann, C.; Patrick, A. D.; Hoyt, H. M.; Lobkovsky, E.; Wieghardt, K.; Chirik, P. J. *J. Am. Chem. Soc.* **2010**, *132*, 15046.
(39) Vidyaratne, I.; Scott, J.; Gambarotta, S.; Duchateau, R. *Organometallics* **2007**, *26*, 3201.
(40) Lagaditis, P. O.; Lough, A. J.; Morris, R. H. *Inorg. Chem.* **2010**, *49*, 10057.
(41) Lagaditis, P. O.; Mikhailine, A. A.; Lough, A. J.; Morris, R. H. *Inorg. Chem.* **2010**, *49*, 1094.
(42) Mikhailine, A. A.; Morris, R. H. *Inorg. Chem.* **2010**, *49*, 11039.
(43) Sui-Seng, C.; Haque, F. N.; Hadzovic, A.; Pütz, A.-M.; Reuss, V.; Meyer, N.; Lough, A. J.; Iuliis, M. Z.-D.; Morris, R. H. *Inorg. Chem.* **2009**, *48*, 735.
(44) Keim, W.; Killat, S.; Nobile, C. F.; Suranna, G. P.; Englert, U.; Wang, R.; Mecking, S.; Schröder, D. L. *J. Organomet. Chem.* **2002**, *662*, 150.
(45) Chien, P. S.; Liang, L. C. *Inorg. Chem.* **2005**, *44*, 5147.
(46) Skinner, M. E. G.; Li, Y. H.; Mountford, P. *Inorg. Chem.* **2002**, *41*, 1110.
(47) King, W. A.; Di Bella, S.; Gulino, A.; Lanza, G.; Fragala, I. L.; Stern, C. L.; Marks, T. J. *J. Am. Chem. Soc.* **1999**, *121*, 355.
(48) Cohen, J. D.; Fryzuk, M. D.; Loehr, T. M.; Mylvaganam, M.; Rettig, S. J. *Inorg. Chem.* **1998**, *37*, 112.
(49) Fryzuk, M. D.; Haddad, T. S.; Mylvaganam, M.; McConville, D. H.; Rettig, S. J. *J. Am. Chem. Soc.* **1993**, *115*, 2782.
(50) Hirotsu, M.; Fontaine, P. P.; Zavalij, P. Y.; Sita, L. R. *J. Am. Chem. Soc.* **2007**, *129*, 12690.
(51) Morello, L.; Ferreira, M. J.; Patrick, B. O.; Fryzuk, M. D. *Inorg. Chem.* **2008**, *47*, 1319.
(52) Morello, L.; Yu, P. H.; Carmichael, C. D.; Patrick, B. O.; Fryzuk, M. D. *J. Am. Chem. Soc.* **2005**, *127*, 12796.
(53) Chirik, P. J.; Henling, L. M.; Bercaw, J. E. *Organometallics* **2001**, *20*, 534.
(54) Pool, J. A.; Lobkovsky, E.; Chirik, P. J. *J. Am. Chem. Soc.* **2003**, *125*, 2241.
(55) Pool, J. A.; Lobkovsky, E.; Chirik, P. J. *Nature* **2004**, *427*, 527.
(56) Kofron, W. G.; Baclawski, L. M. *J. Org. Chem.* **1976**, 1879.
(57) Bergbreiter, D. W.; Killough, J. M. *J. Am. Chem. Soc.* **1978**, *100*, 2126.